

Eta Car through the eyes of interferometers

O. Chesneau¹, R. van Boekel², T. Herbst², P. Kervella³, M. Min⁴,
L.B.F.M. Waters⁴, Ch. Leinert², R. Petrov⁵ and G. Weigelt⁶

¹ Observatoire de la Côte d’Azur-CNRS-UMR 6203, Dept. Gemini, Avenue Copernic, 06130 Grasse, France Olivier.Chesneau@obs-azur.fr

² Max-Planck-Institut für Astronomie, Königstuhl 17, 69117 Heidelberg, Germany

³ LESIA, CNRS-UMR 8109, Observatoire de Paris-Meudon, 5 place Jules Janssen, 92195 Meudon Cedex, France

⁴ Sterrenkundig Instituut ‘Anton Pannekoek’, Kruislaan 403, 1098 SJ Amsterdam, The Netherlands

⁵ Université de Nice-Sophia Antipolis, Parc Valrose, 06108 Nice, France

Summary. The core of the nebula surrounding Eta Carinae has been observed recently with VLT/NACO, VLTI/VINCI, VLTI/MIDI and VLTI/AMBER to constrain spatially *and* spectrally the warm dusty environment and the central object. Narrow-band images at $3.74\ \mu\text{m}$ and $4.05\ \mu\text{m}$ reveal the structured butterfly shaped dusty environment close to the central star with an unprecedented spatial resolution of about 60 mas. VINCI has resolved the present-day stellar wind of Eta Carinae on a scale of several stellar radii owing to the spatial resolution on a scale of 5 mas ($\sim 11\ \text{AU}$) provided by 25m projected baselines. The VINCI observations show that the object is elongated with a de-projected axis ratio of approximately 1.5. Moreover the major axis is aligned with that of the large bipolar nebula that was ejected in the 19th century. Fringes have also been obtained in the Mid-IR with MIDI using baselines of 75m and a peak of correlated flux at 100 Jy level situated $0.3''$ south-east from the photocenter of the nebula at $8.7\ \mu\text{m}$ is detected. This correlated flux is partly attributed to the central object but it is worth noting that at these wavelength virtually all the $0.5'' \times 0.5''$ central area can generate detectable fringes witnessing the large clumping of the dusty ejecta. These observations provide an upper limit for the SED of the central source from $3.8\ \mu\text{m}$ to $13.5\ \mu\text{m}$ and constraint some parameters of the stellar wind which can be compared to the Hillier’s model. Lastly, we present the great potential of the AMBER instrument to study the numerous near-IR emissive lines from the star and its close vicinity. In particular, we discuss its ability to detect and follow the faint companion.

1 Introduction

Eta Carinae is one of the best studied but least understood massive stars in our galaxy ([8]). Eta Car is classified as a Luminous Blue Variable (LBV), a short lasting phase of hot stars evolution characterized by strong stellar winds and instabilities leading to possible giant eruptions. Eta Car offered a unique opportunity to observe the consequences of such a giant events with the two historical eruptions in the 1840s and 1890s.

The large bipolar nebula surrounding the central object, known as the “Homunculus”, was formed during the first one, while some fainter and less

extended structures were attributed to the lesser 1890 event¹. Despite numerous observations and theoretical studies, the cause of the two outbursts remains unknown.

Currently, the Homunculus lobes span a bit less than $20''$ on the sky (or 45000 AU at the system distance of 2.3 kpc) and are largely responsible for the huge infrared luminosity of the system. The central source is therefore deeply embedded and studied only via indirect observations.

Improved spatial resolution observations have often been the key for the progress in our understanding of this emblematic embedded object. The central source has been studied by speckle interferometry techniques in visible light, which revealed a complex knotty structure ([31], [14]). Originally, three remarkably compact objects between $0.1''$ and $0.3''$ northwest of the star were isolated (the so-called BCD *Weigelt blobs*, the blob A being the star itself). Other similar but fainter objects have since been detected ([32]; [7]). They are found to be surprisingly bright ejecta moving at low speeds ($\sim 50 \text{ km.s}^{-1}$). They belong to the equatorial regions close to the star; their separation from the star is typically 800 AU.

Eta Car has been systematically observed with the Hubble Space Telescope (HST) instruments ([7], GHRS; [21], [19], WFPC2/NICMOS; [27], [28], ACS/HRC among many others) and in particular the Space Telescope Imaging Spectrograph (STIS) since beginning of 1998 ([18], [26], [30], [16]). With 0.1 arcsec angular resolution and a spectral resolving power of 5000, the central point-like source can be studied more or less independently from the extended nebulosity and the nebular structures can be dissected (cf. contribution from T. Gull in these proceedings). The central source could be separated from the Weigelt blobs allowing a careful study of the central object by Hillier et al. ([17]). The mostly reflective nebula also allowed an indirect study by STIS of the stellar wind from several points of view at different latitudes in the nebulae by means of reflected P Cygni absorption in Balmer lines ([26]). The authors convincingly prove the asphericity of the wind suggesting that an enhanced polar wind mass-loss.

Eta Car was observed with the Infrared Space Observatory Observatory (ISO, [20]). The ISO spectra indicated that a much larger amount of matter should be present around Eta Car in the form of cold dust than previously estimated. Observations with higher spatial resolution by Smith et al. ([23], [25]) showed a complex but organized dusty structure within the three inner arcseconds. They showed that the dust content in the vicinity of the star is relatively limited and claimed that the two polar lobes should contain the large mass of relatively cool dust necessary to explain the ISO observations (but see [10]). Correlated to these observational uncertainties, the mechanism required to form the two gigantic lobes of gas and dust remains poorly understood.

¹although by that time the dust absorption was such that the opacity around the central was such that the amplitude of this event is not really constrained

One of the main limitation of HST observations is probably that its instruments are mostly restricted to optical domain. The Homunculus is a dusty nebula dominated by reflected starlight at optical wavelengths and even in K band, the scattered light from the central object is far from being negligible. This makes it problematic to really look through all this material without being affected by the diffuse light. Lower extinction in the IR allows us to look inside the Homunculus to study embedded structures, provided that the spatial resolution is sufficient to study them.

In the following, we present the current results obtained by the impressive gain in spatial resolution provided by the VLT with the NACO instrument (Sect.1) and the VLTI with the VINCI (Sect.2) and MIDI (Sect.3) instruments. In Sec.4 we present the potential of AMBER observations for detecting and observing the companion of Eta Car.

2 NACO observations: the inner dusty nebula

The interferometric observations presented in the following sections were complemented with broad- and narrow-band observations taken with the NAOS/CONICA (NACO) imager installed on VLT UT4 (Kueyen), equipped with an adaptive optics (AO) system. These observations are described extensively in van Boekel et al. ([1]) and Chesneau et al. ([2]).

The diffraction limit (defined by the Point Spread Function, PSF of the telescope) of the 8 meter telescope at $3.8 \mu\text{m}$ is about 100 mas. At this wavelength, the NACO adaptive optics is sufficient to correct atmospheric seeing, routinely providing a strehl ratio approaching 0.5. A careful deconvolution procedure can improve the spatial resolution to about 50-80 mas, i.e. close to the diffraction limit of K band images obtained usually with lower strehl performances and more affected by scattered light (see below). These NACO images represent the highest-resolution observations of Eta Car from a single telescope in K and L bands (shown in the Figure 1). They resolve much of the sub-arc second structures.

The NACO observations offer the opportunity to bridge the gap to the interferometric data obtained with very high resolution but sparse UV coverage and they also represent a great help for single mode observations for which the Field-Of-View (FOV) is strongly limited.

Dust plays a key role in the study of Eta Car. It intervenes in every observation as strong and patchy extinction is frequently invoked as an important process in explaining the photometric variability of Eta Car. However, the exact nature and location of dust formation/destruction sites has never been observed. In the close vicinity of the central object, dust is still present in large quantities and even the K band images are contaminated by the intense scattered light which decreases strongly only in L band.

A $3.8 \mu\text{m}$ narrow-band deconvolved image is shown in Fig. 1. This image illustrates the difficulty to observe such a complex and extended object with

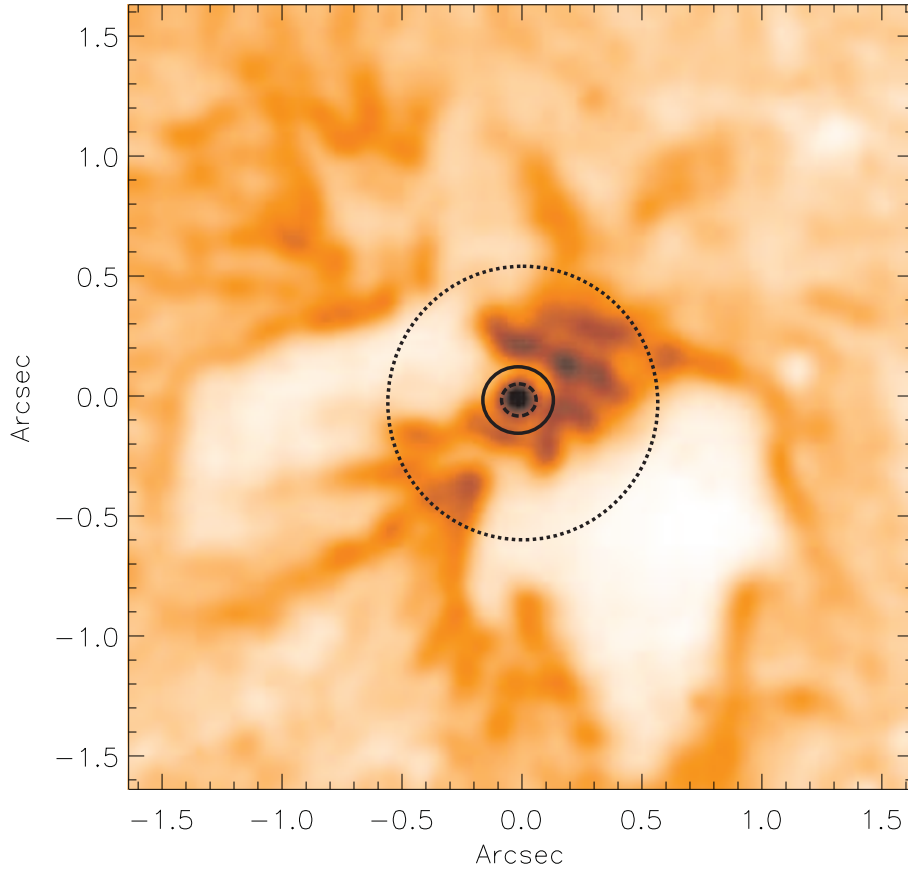


Fig. 1. NACO $Pf\gamma$ deconvolved image. The resolution achieved is in the order of 60 mas. To enhance the contrast, the image $I^{1/4}$ is shown. The FOV of the different interferometric instruments of the VLTI with UTs and ATs are shown: $2.2\mu\text{m}$ with ATs and $10\mu\text{m}$ with UTs in solid line, $2.2\mu\text{m}$ with UTs in dashed line, $10\mu\text{m}$ with ATs in dotted line.

long baseline interferometers. The key difficulty is that all spatial structures at the scale of one Airy disk contribute to the interferometric signal, especially the single mode AMBER and VINCI interferograms. AMBER and VINCI are sensitive to the 1-20 mas structures at the center of the FOV and are "contaminated" by everything inside a complex 100-150 mas patch with the UTs and inside a 400-600 mas patch with ATs at $2.2\mu\text{m}$. This means that the visibility and phase can be contaminated by, for example, the closest regions of the "Weigelt complex". If we want to be fully able to interpret AMBER data, we would have to control accurately the pointing and do mosaicking to explore the inner 30-150 mas scale. The AMBER capability to disentangle between narrow (from blobs) and broad (from central star) emissive lines

owing to its great spectral resolution ($R=10000$) should be used to provide the necessary astrometric information for assessing the pointing quality (see Sect. 5).

For MIDI observations, the situation is even worse since in this case the dust emission flux is several times above the central star one and virtually all the nebula is bright. The airy patterns of UTs and ATs delimit a region of 0.25 and 1.25 arcsec respectively. One advantage although, is the availability of a 3" FOV to get simultaneously fringes from extended regions i.e. non restricted to a single airy disk FOV.

3 VINCI observations: the evidence of rotation

Rotation is an intrinsic property of all stars, which definitely cannot be neglected in the case of early spectral types. The most obvious consequence is the geometrical deformation that results in a radius larger at the equator than at the poles. Another well established effect, known as gravity darkening or the von Zeipel effect, is that both the surface gravity and emitted flux decrease from the poles to the equator. Although well studied in the literature, such effects of rotation have rarely been directly tested against observations.

It must be pointed out that in the case of Eta Car, the wind density is such that the true photosphere is not visible. Therefore, the consequences of rotation can only be indirectly observed through their effects on the dense wind of this star. The common thought was until recently that centrifugal forces favor mass-loss in the equatorial plane until the indirect observations of Smith et al. ([26]). We will see in the following that interferometry is the most appropriate tool to detect directly the asymmetry of the central source.

The VINCI observations of Eta Car are described in van Boekel et al. ([1]). The two 35 cm siderostats and the instrument VINCI were used to obtain interferometric measurements at baselines ranging from 8 to 62 m in length. The observations were carried out in the first half of 2002 in four different nights, and again in early 2003. The baselines used, have a ground length of 8, 16, 24, and 66 m respectively. In particular observations with the 24 m baseline cover a wide range of projected baseline orientations.

VINCI observations provide information on the K continuum from the central object, the flux from emissive lines being limited to less than a few percent of the total flux in this band. As mentioned in the previous section, a good accuracy of pointing from siderostats was required for such a study. Indeed, their extended FOV includes in addition to the central source (representing 57% of the observed flux), the regions from the 'Weigelt complex' within the dotted curve in Fig.1. AMBER should be used to evaluate potential measurements biases.

VLTI/VINCI observations clearly resolve this central object; its size can now be measured to be 5 mas at 2 μm corresponding to 10 AU at the distance of Eta Car. This is much larger than the stellar photosphere so that we must

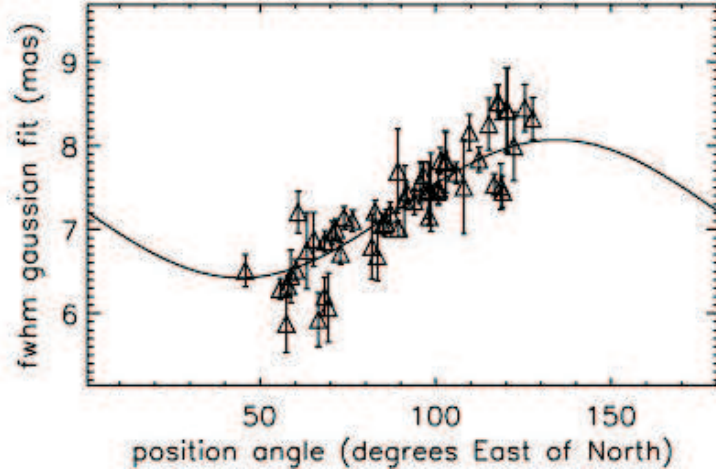


Fig. 2. Variation of FWHM fitted to the visibilities measured with VINCI as a function of projected orientation of the 24 m baseline. The solid line gives the best fit to the measurements, assuming a 2D Gaussian shape of the source at each projected baseline orientation. The amplitude of the size variations gives a ratio of major to minor axis of 1.25 ± 0.05 . The major axis has a position angle of $134^\circ \pm 7^\circ$ East of North.

be observing the radius at which the stellar wind becomes opaque. The radiation is dominated by free-free emission and electron scattering; the radius of the surface is determined by the mass-loss rate and the wind clumping factor. The diameter measurement with the VLTI breaks the degeneracy between these two parameters in previous modeling efforts; mass loss rate and clumping factor can be derived separately from the combination of HST/STIS spectroscopy with the interferometric data. These observations are consistent with the presence of one star which has an ionized, moderately clumpy stellar wind with a mass loss rate of about $1.6 \times 10^{-3} M_\odot \text{ yr}^{-1}$. This star-plus-wind spherical model, developed by Hillier et al. ([17]), is also consistent with the HST STIS observations of the central object.

A second important conclusion from the VLTI data is that the central object is not spherically symmetric, the star is elongated with a de-projected axis ratio of about 1.5. Moreover, its major axis is aligned with that of the large-scale structure. These VLTI observations give an important confirmation of the wind geometry previously proposed by Smith et al. ([26]). This alignment on all scales means that the 1840 outburst looks like a scaled-up version of the present-day wind, and that this wind is stronger along the poles than in the equatorial plane. As Dwarkadas & Owocki ([12]) showed, the radiation pressure in these massive stars is stronger in the polar regions because of the von Zeipel effect. The wind is primarily controlled by this phenomenon and not by the local gravity.

4 MIDI observations: dusty clumps, everywhere!

The MIDI recombiner attached to the VLTI is the only instrument that is able to provide sufficient spatial and spectral resolution in the mid-infrared to disentangle the central components in the Eta Car system from the dusty environment. The Hillier model suggests a flux level at $10\ \mu\text{m}$ of 200-300 Jy and 10-15 mas diameter of the star plus wind at this wavelength.

Eta Car was observed with MIDI with the UT1 and the UT3 telescopes during commissioning and guaranteed time observations. These observations are shown in Chesneau et al. ([2]). Virtually all the capabilities of MIDI were used during these 4h observations: single-dish imaging capabilities during acquisitions, spatially resolved long slit spectroscopy, undispersed map of the correlation pattern and finally dispersed fringes, all data taken within the small, but indeed of great interest, $3''$ FOV of the instrument.

The spatial distribution of the fringes detected by MIDI with the $8.7\ \mu\text{m}$ filter is shown in Fig.3. The peak of the fringes is localized at the position of the star itself but an extended halo is also visible in the Weigelt complex about $0.4\text{-}0.6''$ northwest from the star. This is the confirmation that highly compressed material emitting strongly at $8.7\ \mu\text{m}$ exists in this region. The the fringes at the location of the Weigelt blobs are definitely more extended than a single PSF FWHM at $8.7\ \mu\text{m}$ (220 mas).

This implies that in the equatorial Weigelt region a fraction of the dust is embedded in clumps with a typical size smaller than 10-20 mas (25-50 AU) within a total extent of about 1000 AU. Nevertheless, this correlated flux represents only a few percent of the total flux at these locations. It must be pointed out that only a few scans with fringes have been recorded during this commissioning measurement and the lowest detectable fringe signal visible in Fig. 3 is about 20 Jy. With more integrated frames it should be possible to see that all the Weigelt complex indeed can generate fringes.

Dispersed fringes were also obtained which reveal a correlated flux of about 100 Jy situated $0.3''$ south-east of the photocenter of the nebula at $8.7\ \mu\text{m}$, which corresponds with the location of the star as seen in NACO images. This correlated flux is partly attributed to the central object, and these observations together with the VINCI ones provide an upper limit for the SED of the central source from $2.2\ \mu\text{m}$ to $13.5\ \mu\text{m}$ (Fig. 4).

The 74m baselines were roughly perpendicular to the main axis of the nebula and indeed the prolate star itself. This means that the baselines were oriented perpendicular to the main stellar axis, where the star is smaller, corresponding to a maximum correlated flux. Hence, the MIDI measurements can be considered as an upper limit of the correlated flux observable from the star. The MIDI correlated flux, despite large error bars is obviously below the model prediction. We note also that the MIDI data were acquired at the

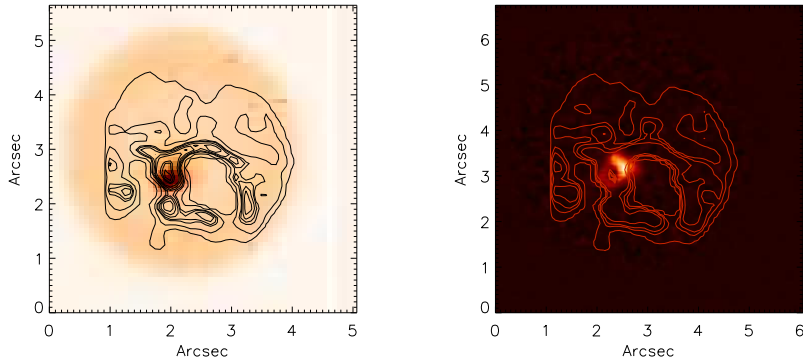


Fig. 3. Left, the figure shows the signal fluctuations within the MIDI acquisition FOV. The external regions are dominated by the detector noise and the internal regions by the tunnel and sky background fluctuations. The signal from the fringes is strong and centered on the position of the star as seen in the Fig.1 image. The contour plot represents the contours of the deconvolved MIDI $8.7 \mu\text{m}$ acquisition image. Right, the noise pattern and the fringe pattern from a calibrator have been subtracted from the previous figure in order to show the extended fringe signal. The vertical orientation is approximately parallel to the bipolar nebula ($\text{PA}=138^\circ$).

periastron passage of the faint companion (still undetected), and no emission lines in the extracted spectra is visible compared to the model².

Nine spectrally dispersed observations from the nebula itself at $\text{PA}=318$ degree, i.e. in the direction of the bipolar nebula within the MIDI field of view of $3''$ were also extracted. A large amount of corundum (Al_2O_3) is discovered, peaking at $0.6\text{-}1.2''$ south-east from the star, whereas the dust content of the Weigelt blobs is dominated by silicates. These observations are extensively discussed in Chesneau et al. ([2]).

The Guaranteed Time Observations presented here were intended to judge the feasibility of MIDI observations of Eta Car. The observations, conducted with UTs only, demonstrated the interest of such a scientific program but also the difficulty to extract the central star signal from the dust one. The results were obtained with only one baseline and at periastron. In particular, a possible explanation of the low correlated flux observed compared with the model of Hillier could be the presence near the central star of the wind-

²The whole Eta Car spectrum is dominated by strong emission lines which disappear during a short time at periastron passage. Despite the low spectral resolution of MIDI ($R=30$ with the prism), we can clearly say that these lines were absent for these observations. The emission lines are for instance well detectable by for the HD316285, a twin of Eta Car from the spectral point of view, with the same spectral resolution.

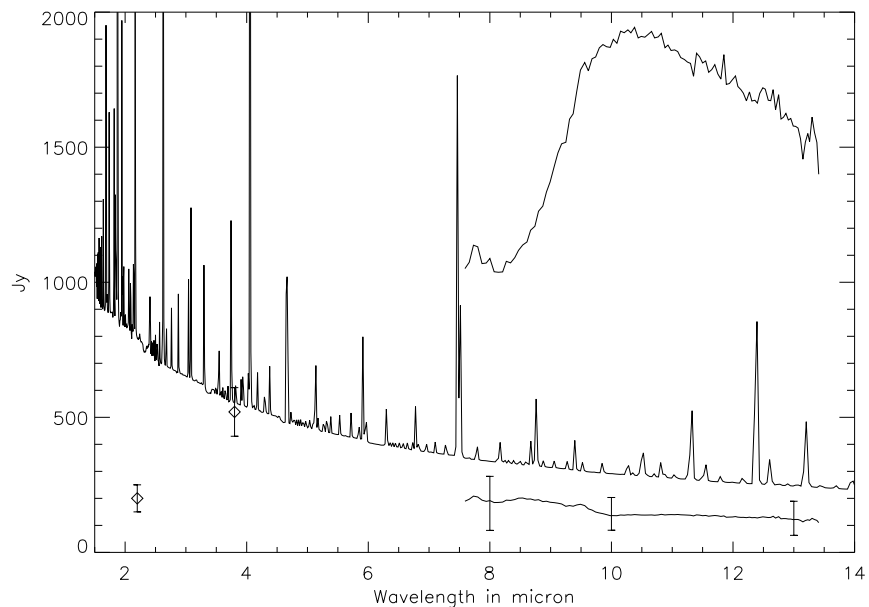


Fig. 4. Spectral energy distribution from the Hillier's model compared with the photometry extracted from an airy disk centered on the star (upper curve) and the extracted correlated flux (lower curve). The near-IR photometry in K and L band are also indicated.

wind collision zone, commonly thought to be the place of an intense dust formation. The Guaranteed Time with UTs is now completed and the star is offered for open time observations. It would be of great interest now that the orbital phase is near apastron, to undertake a more ambitious program with UTs taking advantage that AMBER is ready to perform contemporary observations. Some test observations are also planned to check the feasibility of a large observing program with ATs. Their large FOV could prevent the extraction of pertinent information for such a complex object but they also offer a wealth of baselines which could allow a good uv coverage.

5 AMBER observations: revealing the binary?

The original detection of a 5.52 year period in Eta Carinae in the spectroscopic and near-infrared photometric data of Daminieli ([4]) has been confirmed by later observations ([6], [9], [33]). The existence, mass, and orbit of a companion and its possible impact on the behavior of the primary are still strongly disputed (e.g. [9]; [3], [15], [22]; [11]).

The deduced parameters of the orbit from X-ray observations by Corcoran et al. ([3]) imply that the periastron and apastron distances are roughly 1.5 AU and almost 30 AU, respectively (see also [22]). At closest approach, the secondary is well embedded, deep within the dense wind of the B-star primary.

The first observations of Eta Car by Amber appear promising (see Petrov et al., this volume). Already, absolute and differential visibilities, differential and closure phases were obtained at medium (R=1500) and high (R=10000) spectral resolution. Even with this impressive amount of information, the spatial interpretation of this complex (and time variable) object remains limited by the poor uv coverage. We advocate a spectroscopic approach based on the study of the numerous near-infrared lines formed at different spatial location, viewing the central star through different angles and experiencing different excitation mechanisms (cf. in particular Smith et al. 2002b, Fig.14 and Fig.15).

Near-infrared emission lines are unique diagnostics of the geometry and kinematics the wind of Eta Car and for studying in close vicinity. The infrared spectrum is a strong function of position in Eta Car's nebula, with molecular hydrogen and [FeII] tracing more easily cold or collisionally excited material formed in the circumstellar outside the inner 1" region ([24], [29]). The HeI λ 10830 line is of particular interest, emitted from some equatorial ejecta ([24]). A. Daminieli has been monitoring HeI λ 10830, Pa γ and Pa δ over the past several years and showed that this line is very sensitive to the orbital motion of the companion ([4], [5], see also the web site of A. Daminieli <http://www.etacarinae.iag.usp.br/>).

Smith ([24]) was able to marginally resolve the mission from the Weigelt blobs, allowing their combined spectrum to be separated from the central star for the first time at IR wavelengths. This effect has been immediately evidenced during the first AMBER observations: narrow emission lines are offset from the star's position by 0.2 to 0.4 arcsec, while the broad lines from the star wind appear when the telescope is accurately pointed. Thus, it should be possible to separate these blobs from the star by extracting segments along the slit on either side of the star's position. To the NW the emission is dominated by the blobs, and to the SE the star dominates.

The search of any indices able to constrain the companion is now intensively conducted. By studying the high and low state of excitation from the emission lines of Weigelt blobs, found consistent results ([30]) with an O supergiant or a Wolf-Rayet (W-R) star. Falceta-Goncalves et al. ([13]) recently studied the accumulation of material in the wind-wind collision zone in an at-

tempt to conciliate X-rays and optical observations. They also considered the formation rate of dust in the collision zone and were conducted to interesting conclusions, complementary to the MIDI observations ones by Chesneau et al. ([2]). Their Fig.3, showing the expected tail of gas and dust created in the collision zone illustrates the potential complexity of the object observed soon intensively with AMBER.

References

1. van Boekel, R., Kervella, P., Schöller, M., et al., *A&A*, **410**, L37 (2003)
2. Chesneau, O., Min, M., Herbst, T. et al., *A&A*, **435**, 1043 (2005)
3. Corcoran, M.F., Ishibashi, K., Swank, J.H., Petre, R., *ApJ* **547**, 1034 (2001)
4. Daminieli, A., *ApJ Letters*, **460**, L49, (1996)
5. Daminieli, A., Conti, P.S., Lopes, D.F., *New Astronomy*, **2**, 107 (1997)
6. Daminieli, A., Kaufer, A., Wolf, B., Stahl, et al. *ApJ Letters*, **528**, L101 (2000)
7. Davidson K., Ebbets, D., Morse, J.A. , *AJ*, **113** 335 (1997)
8. Davidson K. & Humphreys, R.M., *Annu. Rev. Astron. Astrophys.*, **35**, 1 (1997)
9. Davidson K., Ishibashi, K., Gull, T.R. et al., *ApJ* **530**, L107 (2000)
10. de Koter, A., Min, M., van Boekel, R., Chesneau, O., *ASPC*, **332**, 319 (2005)
11. Duncan, R.A. & White, S.M., *MNRAS*, **338**, 425 (2003)
12. Dwarkadas, V.V. & Owocki, S.P., *ApJ*, **581**, 1337 (2002)
13. Falceta-Gonçalves, D., Jatenco-Pereira, V., Abraham, Z., *MNRAS*, **357**, 895 (2005)
14. Falcke, H., Davidson, K., Hofmann, K.-H., Weigelt, G., *A&A*, **306**, L17 (1996)
15. Feast, M., Whitelock, P., Marang, F., *MNRAS*, **322**, 741, (2001)
16. Gull, T.R., Vieira, G. and Bruhweiler, F., *ApJ*, **620**, 442 (2005)
17. Hillier, D.J., Davidson, K., Ishibashi, K., Gull, T., *ApJ*, **553**, 837 (2001)
18. Ishibashi, K., Gull, T.R., Davidson, K. et al., *ApJ*, **125**, 3222 (2003)
19. King, N.L., Nota, A., Walsh, J.R. et al. *ApJ*, **581**, 285 (2002)
20. Morris, P.W., Waters, L.B.F.M., Barlow, M.J. et al., *Nature*, **402**, 502 (1999)
21. Morse, J.A., Davidson, K., Bally, J. et al., *AJ*, **116**, 2443 (1998)
22. Pittard, J.M., Corcoran, M.F., *A&A*, **383**, 636 (2002)
23. Smith, N., Gehrz, R.D., Hinz, P.M. et al., *ApJ*, **567**, L77 (2002a)
24. Smith, N., *MNRAS*, **337**, 1252 (2002b)
25. Smith, N., Gehrz, R.D., Hinz, P.M. et al., *AJ*, **125**, 1458 (2003a)
26. Smith, N., Davidson, K., Gull, T.R. et al., *ApJ*, **586**, 432 (2003b)
27. Smith, N., Morse, J.A., Gull, T.R., et al., *ApJ*, **605**, 405 (2004a)
28. Smith, N., Morse, J.A., Collins, N.R. and Gull, T.R., *ApJ*, **610**, L105 (2004b)
29. Smith, N., *MNRAS*, **357**, 1330 (2005)
30. Verner, E., Bruhweiler, F., Gull, T.R., *ApJ*, **624**, 973 (2005)
31. Weigelt, G. & Ebersberger, J., *A&A*, **163**, L5 (1986)
32. Weigelt, G. Albrecht, R., Barbieri, C. et al., *RMxA&A, Ser. Conf.*, **2**, 11 (1995)
33. Whitelock, P.A., Feast, M.W., Marang, F. et al., *MNRAS*, **352**, 447 (2004)